

Influence of the Synthesis Parameters in CNT Doped with Nitrogen Towards the Electroreduction of Oxygen

Isaías Zeferino González, Ivonne Alonso Lemus, Beatriz Escobar Morales, Ana María Valenzuela Muñiz, Ysmael Verde Gómez^a

^a Instituto Tecnológico de Cancún, Av. Kabah Km. 3, Cancún, Q.R., México, 77500. yverde@yahoo.com

ABSTRACT

One of challenges in the commercialization of fuel cells is the high cost and scarcity of platinum based catalysts. In addition, there is also the slow kinetics problem in the oxygen reduction reaction (ORR). Therefore, alternative electrocatalysts are needed. Systems based on doped carbon nanostructures (without the use of active metals) have been proposed as a good option to solve both of the drawbacks before mentioned. In the present study, nitrogen doped carbon nanotubes (N-CNTs) were synthesized by a modified chemical vapor deposition method. Pyridine was used as carbon and nitrogen precursor and ferrocene as a metal catalyst for the nanotubes growth. Different synthesis conditions such as temperature of the reactor, carrier gas flow, concentration of the reactants, and vaporizer temperature were studied. The purpose of this parameters variation was to figure out the optimal conditions in which the material achieves the best catalytic activity. The electrocatalytic performance was evaluated towards the ORR by linear sweep voltammetry measurements. A catalyst-coated rotating disk electrode at different rotation rates in 0.5 M H₂SO₄ solution was performed. The results show that the reactor temperature and gas flow had a significantly influence in the materials characteristics and hence the electrocatalytic activity for ORR. The factors that determine the high electrocatalytic activity for ORR of the N-CNTs are discussed.

Keywords: Nanotubes; Carbon; Synthesis.



1. Introduction

The fuel cell uses precious metals in the electrodes to carry out the reactions. Traditionally, Platinum is the best known electro-catalyst for the reaction of oxidation and reduction. However, scarcity, high price and degradation of platinum as a catalyst in the fuel cell represent a challenge to be overcome [1, 2]. In recent years, it has been efforts to reduce the platinum loading on the electrodes of the cell. However, the lack of this noble metal follows the trend of consumption. Therefore, it is necessary to develop new catalytic materials available, cheap and effective to replace Pt based electrocatalysts.

Carbon nanotubes doped with nitrogen have been considered as alternative catalysts for oxygen reduction reaction (ORR) in the cathode electrode of the fuel cell [3]. There are many studies concerning to the synthesis of carbon nanotubes doped with nitrogen atoms using different carbon-nitrogen precursor by chemical vapour deposition (CVD) method. It has been shown that these materials have high electro-catalytic activity for ORR. Alexeyeva et al. [4] synthesized N-CNTs using acetonitrile as carbon and nitrogen source. They studied the ORR in acid media where analyzes reveal that the nitrogen content in the wall of the nanotubes shows significant activity than nanotubes without doping. Higgins et al. [5] synthesized carbon N-CNTs by CVD method using three different precursor solutions: Ethylenediamine (ED), 1,3-diaminopropane (DAP) and 1,4-diaminobutane (DAB). Their results showed that the precursor solutions which have a higher nitrogen atomic ratio in the N-CNTs yielded better oxygen reduction. The N-CNTs prepared with ED had a nitrogen content of 4.75 at. % and showed a superior activity of ORR than the DAP (2.48 at. %N) and the DAB (1.20 at.% N). Wong et al. [2] obtained N-CNTs through CVD using aniline, diethylamine (DEA) and ethylenediamine (EDA). Analysis reveals that the N-CNTs obtained from EDA (6.58 at. % N) was the most active sample for ORR in acidic media than aniline (5.99 at. % N) and DEA (4.33 at.% N). Xiong et al. [6] synthesized N-CNT via modified CVD using melamine and urea as different nitrogen precursors. The N-CNTs resulting from the melamine (4.55 at. % N) showed higher performance than urea (2.20 at. % N) for ORR. These studies show the important role of nitrogen precursors on the structure of the N-CNTs.

Several N-CNTs studies have been carried out evaluating not only the effect of the nitrogen precursors but also the nitrogen concentration at different C/N ratio. Nevertheless, a few studies have been made on effect of the different synthesis conditions of N-CNTs on the ORR. This work presents the effect of various parameters such as reactor temperature, carrier gas flow rate, concentration of the reactants, and vaporizer temperature over the physical, chemical and electrochemical properties of N-CNTs synthesized with pyridine as nitrogen and carbon source.

2. Experimental

2.1 N-CNTs synthesis

N-CNTs synthesis was carried out by a simple and modified chemical vapour deposition process. Pyridine (99.5%, Merck) was used as carbon and nitrogen source and ferrocene (98%, Aldrich) as a metal catalyst for the nanotubes growth. Vycor tubes (0.7 cm internal diameter and 50 cm length) were utilized as substrate and it was placed into a tubular furnace (Lindberg/blue). Synthesis was carried out by heating



the tube and injecting the precursor solution under argon atmosphere. After the synthesis process the furnace was cooled down at room temperature under argon gas flow. The final products were obtained from Vycor tube substrate. N-CNTs were treated with concentrated nitric acid (66.5%, J.T. Baker) for 12 h. Four factors were changed during the synthesis process, each one with two levels. The factors and the nomenclature used is showed in Table 1. 16 experiments were carried out to study the effect of the factors on the electrocatalytic performance of the N-CNTs.

Table 1. Synthesis parameters of N-CNTs

FACTORS	LEVEL	
	Low	High
Solution concentration (g/L)	18 [Y]	36 [X]
Argon gas flow rate (L/min.)	0.5 [B]	1 [A]
Vaporizer temperature (°C)	180 [180]	200 [200]
Reactor temperature (°C)	800 [8]	900 [9]

2.2 Physical and chemical characterization

The Scanning electron microscope (SEM) Vega 3 Tescan was used to study the morphology and topology of the materials. The samples were placed on the copper strips, supported on the sample holder of the microscope. Images were acquired from different areas of the sample, in order to assess their average characteristics. The SEM was also used to determine the elemental composition of the sample by energy-dispersive X-ray spectroscopy (EDS). High Resolution Transmission Electron Microscopy (HRTEM) characterization was carried out on JEOL JEM-2200FS microscope to provide nanoscale images of the samples. For HRTEM analysis, the samples were dispersed in ethanol by sonication and then placed on copper grid support. X Ray diffraction was obtained using a D8 Advanced (Bruker), operated at 40kV and 40 mA. Cu-K α radiation was used with a wave length $\lambda = 1.5418 \text{ \AA}$. Raman spectroscopy (LabRAM He-Ne laser 632.8 nm with resolution of 1 cm^{-1}) was utilized in order to investigate the first order Raman scattering of the samples and determine the degree of structural defects present.

2.3 Oxygen reduction reaction activity evaluation

Electrochemical evaluation was carried out in a rotating disk electrode (RDE) using a BASi at different rotation speeds, connected to an Epsilon, whose response was analyzed on a computer with EpsilonEC-200-XP software. The electrochemical cell has three electrodes immersed in a 0.5 M H₂SO₄ solution. The electrodes that were used are: a glassy carbon as working electrode, with a geometric area of 0.07 cm², a reference electrode of Ag/AgCl in saturated 3 mol L⁻¹ KCl and a platinum wire as counter electrode. Catalyst ink prepared with 5 mg N-CNT mixed with 0.5 mL of ethanol and 30 μL Nafion solution was set in ultrasound bath for 1 h. 20 μL of catalyst ink was deposited on the glassy carbon electrode surface and was subsequently slowly dried at room temperature. The working electrode potential was swept from -0.2 to 1 V vs. Ag/AgCl at a scan rate of 5 mV s⁻¹. Before the test, the electrolyte was saturated with argon gas and a potential sweep was performed in order to obtain a background reading. After the background scan, oxygen gas was introduced to saturate the solution. The experiments were performed at the same scan rate



with different working electrode rotation speeds. All potential values reported are referred to the standard hydrogen electrode (SHE).

3. Results and discussion

The estimated amount of N-CNT samples is reported in table 2. The weight average values of the samples indicate that larger amounts of samples were obtained at 900 °C than N-CNT at 800 °C. On the other hand, using SEM micrographs the N-CNTs morphology was studied. Figure 1 shows micrographs of the synthesized nanotubes a) at 800 °C and b) at 900 °C. Analysis indicates that N-CNTs are well-aligned and uniformly distributed on the support. The nanotubes obtained at 800°C have length between 12 and 24 μm , while the nanotubes at 900°C have some hundreds of μm (except sample 200NNBY9). Thus, when the length of nanotubes is higher also the amount of N-CNTs is increased. Therefore, the length of the nanotubes is a parameter that can be associated with quantity.

Table 2. Yield of N-CNTs synthesis.

N-CNT 800 °C			N-CNT 900 °C		
Sample	Length (μm)	Weight (mg)	Sample	Length (μm)	Weight (mg)
180NNBY8	24.60 \pm 4.88	183.20	180NNBY9	100.00 \pm 7.91	526.33
180NNAX8	12.77 \pm 0.55	115.50	180NNAX9	132.80 \pm 11.08	811.29
200NNBY8	13.97 \pm 2.20	98.53	200NNBY9	38.80 \pm 3.96	615.48
200NNAY8	21.84 \pm 2.41	104.81	200NNAY9	126.72 \pm 5.06	765.35
200NNAX8	20.50 \pm 1.36	148.00	200NNAX9	110.85 \pm 5.31	630.89



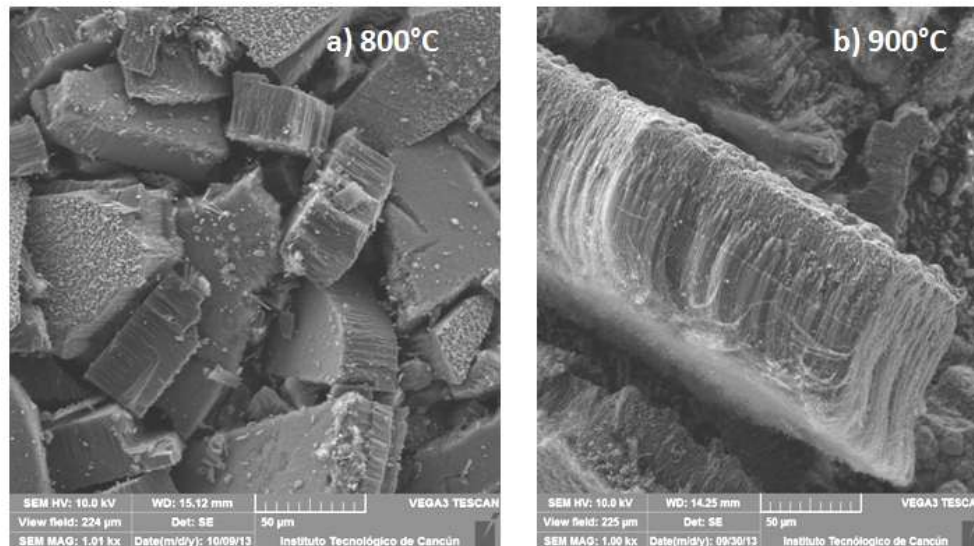


Figure 1. SEM micrographs of N-CNTs at a) 800 °C and b) 900 °C.

Morphology of the materials was also studied by HRTEM (Figure 2). As it can see multiwall carbon nanotubes were obtained with a typical bamboo-like structure; it is common feature observed after incorporation of the nitrogen into carbon lattice, which indicates that the nanotubes are doped with nitrogen [7]. The outer diameter of the carbon nanotubes was estimated, the average values are showed in table 3. The N-CNT at 900°C had higher average outer diameter (84 ± 23 nm) than the N-CNT at 800°C (59 ± 8 nm).

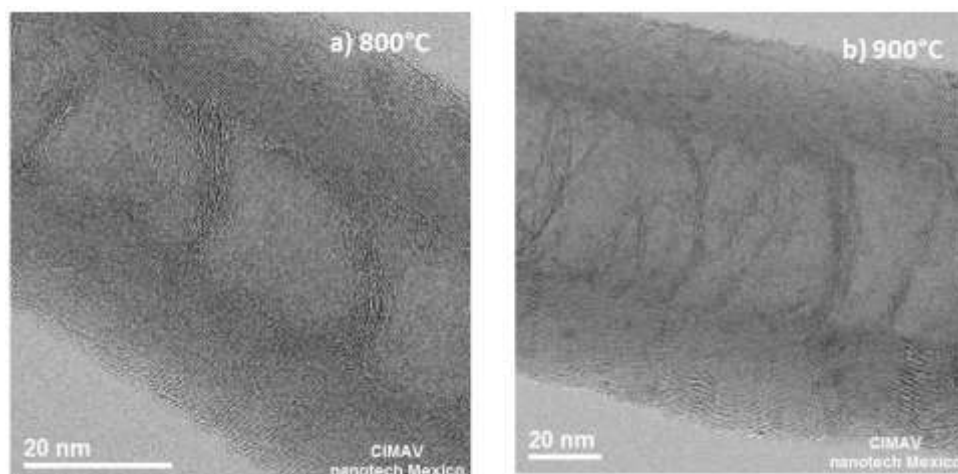


Figure 2. High Resolution Transmission Electron Microscope micrographs of N-CNTs at a) 800 °C and b) 900 °C.

Table 3. Evaluation of the external diameter of the N-CNTs.

N-CNTs at 900°C		N-CNTs at 800°C	
Sample	Diameter (nm)	Sample	Diameter (nm)
180NNBY9	96.36 ± 11.81	180NNBY8	53.64 ± 21.11
200NNAY9L	80.00 ± 33.17	200NNAY8L	64.00 ± 13.42
200NNAX9L	86.04 ± 38.52	200NNAX8L	62.26 ± 3.60
180NNAX9L	75.45 ± 13.89		
200NNBY9L	83.89 ± 20.43		

Table 4. Elemental composition obtained by SEM-EDS.

Sample	C	Fe	N	O
	at. %	at. %	at. %	at. %
180NNBY8	79.14 ± 1.31	0.55 ± 0.14	4.95 ± 0.79	13.12 ± 1.69
180NNBX8	85.43 ± 0.59	0.3 ± 0.05	5.1 ± 0.71	7.83 ± 0.23
180NNAY8	82.7 ± 0.66	0.28 ± 0.04	4.62 ± 0.76	10.93 ± 0.35
180NNAX8	82.82 ± 0.41	0.23 ± 0.02	4.29 ± 0.48	11.75 ± 0.13
200NNBY8	80.48 ± 3.86	0.18 ± 0.06	5.43 ± 2.11	7.88 ± 1.27
200NNBX8	83.66 ± 0.74	0.16 ± 0.01	5.45 ± 0.54	9.45 ± 0.62
200NNAY8	87.97 ± 0.48	0.42 ± 0.02	4.29 ± 0.39	6.42 ± 0.72
200NNAX8	82.03 ± 0.5	0.3 ± 0.06	4.17 ± 0.47	12.48 ± 0.31
180NNBY9	86.31 ± 0.86	0.25 ± 0.02	4.86 ± 0.49	7.2 ± 0.27
180NNBX9	86.22 ± 0.56	0.34 ± 0.04	5.53 ± 0.41	6.9 ± 0.18
180NNAY9	84.63 ± 0.55	0.6 ± 0.13	5.25 ± 0.65	8.19 ± 0.48
180NNAX9	84.57 ± 0.59	0.87 ± 0.24	5.01 ± 0.58	8.13 ± 0.7
200NNBY9	87.49 ± 0.54	0.55 ± 0.09	4.91 ± 0.47	5.94 ± 0.27
200NNBX9	87.97 ± 0.35	0.3 ± 0.05	3.99 ± 0.18	7.16 ± 0.26
200NNAY9	84.55 ± 0.63	0.36 ± 0.04	5.6 ± 0.28	8.55 ± 0.25
200NNAX9	84.79 ± 0.72	0.48 ± 0.07	6.09 ± 0.7	7.15 ± 0.36

The elemental atomic composition analysis of carbon, iron, nitrogen and oxygen by SEM-EDS are showed in Table 4. Analysis demonstrates that nitrogen was successfully incorporated into the structure of the nanotube. SEM-EDS analyses revealed that the content of nitrogen in the nanotubes were slightly different between N-CNT at 900 °C (5.15±0.62 at. %) and N-CNT at 800 °C (4.78±0.51 at. %). On the



other hand, comparison of averages values of the N-CNTs at 900 °C indicate that the synthesized nanotubes with flow 1 L/min. nitrogen content (5.48 ± 0.55 at. %) was higher than 0.5 flow L/min. (4.82 ± 0.38 at. %)

Figure 3 shows of X-ray diffraction patterns obtained from the N-CNTs. It has also been included the pristine CNT for comparisons. Diffraction patterns exhibit intensity 2H graphite phase, which is associated with the formation of N-CNTs multiwall. The first peak located approximately at 26° corresponds to the carbon (002) which forms the hexagonal shape of the graphite. Other peaks located at 42.5° , 44.5° and 53.9° correspond also to the crystallographic planes of graphite at (100), (101) and (004) respectively [8]. The peaks marked with an asterisk (*) correspond to iron carbide (Fe_3C) [9]. In the diffraction pattern was also found Fe_2O_3 located 43.5° (+). The iron comes from residual catalytic agent, unreacted and oxidized during sample handling [10, 11]. The peak around 18° (x) corresponds to SiO_2 , which comes from the residual Vycor tube. The diffraction peaks of the N-CNTs are slightly displaced to the right with respect to the diffraction patterns of the CNT pristine, which could be attributed to the distortion in the crystal lattices and the vacancies caused by the introduction of nitrogen atoms into the carbon networks. Besides, the intensity of diffraction peaks of the N-CNTs in the plane (002) are obviously weaker than that of virgin CNT, because structural defects of carbon nanotubes [12].

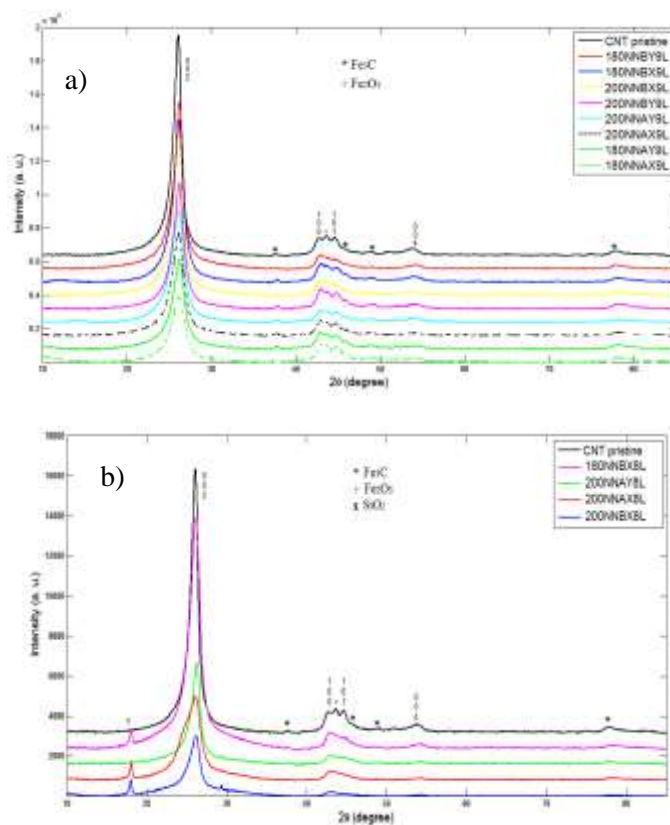


Figure 3. XRD patterns of CNT pristine and N-CNTs at a) 900 °C and b) 800 °C.



Raman spectroscopy was performed in order to obtain information about the crystallinity of the N-CNTs. Figure 4 shows two main peaks around 1333 cm^{-1} and 1588 cm^{-1} corresponding to the D band and G band respectively. The D band is known as the band of disorder, which is caused by the atomic displacement and lattice defects. While the G band indicates the formation of nanotubes well graphitized [13]. The ratio I_D/I_G close to zero suggesting that carbon has a high ordered structure; while a high ratio indicates more defects present in the carbon nanotubes [14, 6]. Analysis of intensity ratio I_D/I_G shown in Table 5 demonstrates that N-CNTs synthesized at $900\text{ }^{\circ}\text{C}$ showed higher structural disorder than $800\text{ }^{\circ}\text{C}$; it can be attributed to the incorporation of nitrogen into the carbon lattice. Another important factor affecting the N-CNTs structure is the argon gas flow; N-CNTs synthesized with low flow (0.5 L/min.) have greater structural defects than carbon nanotubes with high flow (1 L/min.).

The G' band (or 2D) around 2657 cm^{-1} is an overtone of the D band. The intensity ratio $I_{G'}/I_G$ measures the average degree of crystalline perfection [15, 16]. The intensity ratio $I_{G'}/I_G$ shows that the smoothing of N-CNTs decreases considerably with respect to CNT pristine, which can be caused by the incorporation of nitrogen into the carbon.

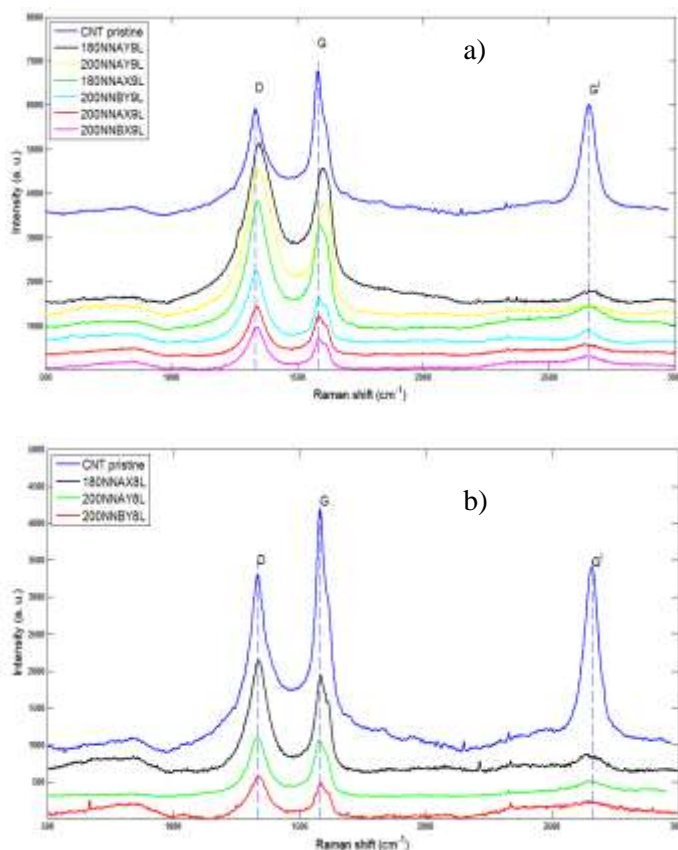


Figure 4. Raman spectra of CNT pristine and N-CNTs at a) $900\text{ }^{\circ}\text{C}$ and b) $800\text{ }^{\circ}\text{C}$.



Table 5. I_D/I_G and I_G/I_G ratio from Raman spectra of N-CNTs.

Sample	I_D/I_G	I_G/I_G
200NNBY9L	1.44 \pm 0.11	0.45 \pm 0.13
200NNBX9L	1.34 \pm 0.01	0.51 \pm 0.06
180NNAY9L	1.25 \pm 0.06	0.18 \pm 0.07
200NNAX9L	1.25 \pm 0.04	0.37 \pm 0.05
200NNAY9L	1.24 \pm 0.05	0.14 \pm 0.02
180NNAX9L	1.19 \pm 0.03	0.21 \pm 0.03
CNT pristine	0.7 \pm 0.04	0.83 \pm 0.07

200NNBY8L	1.29 \pm 0.17	0.5 \pm 0.13
200NNAY8L	1.07 \pm 0.08	0.22 \pm 0.02
180NNAX8L	1.15 \pm 0.02	0.28 \pm 0.09

Linear sweep voltammetry was used to evaluate the electrochemical performance of the N-CNTs. Figure 5 show the polarization curves for the electrochemical reduction of molecular oxygen. As expected, undoped CNT (CNT pristine) is not an active catalyst for ORR. The data show that the limiting current density is not formed in the range of potential studied as it has been know for unmodified carbon materials [4]. Moreover, the analysis of polarization curves was found that the initial potential of the most N-CNTs samples is about 1.15 V/SHE, which is a higher value of 1.11 V/SHE corresponding to commercial 20 wt. % Pt/C. It was noted that the initial potential shifted slightly with temperature variation. This indicates that N-CNTs possess good electrocatalytic activity for the ORR. On the other hand, the N-CNTs synthesized at 900 °C exhibited a limit current density higher than the N-CNTs at 800 °C. This is a clear indication that the N-CNTs (with higher nitrogen amount) at 900 °C showed better electrocatalytic activity. The effect of temperature on the catalytic activity of the N-CNTs has already been reported in the literature [12, 17, 18]. On the other hand, the results of ORR are consistent with the HRTEM micrographs where the nanostructure morphology allow the easy and higher contact with oxygen. Also the high temperature during the synthesis could cause higher nitrogen doping into the carbon nanotubes, having as result a higher ORR activity, which it is in agree with EDS analysis.

N-CNTs sample synthesized under the gas flow to 1 L/min at 900 °C showed higher electrocatalytic activity compare with samples at 0.5 L/min. This analysis revealed that argon gas flow significantly influenced the electrocatalytic properties of N-CNTs. Normally a CVD process, the carrier gas is used to feed precursor sources and catalyst in the reactor. As has been little research on the effect of the flow rate of the carrier gas in the nanotubes formation. Chaisitsak et al. synthesized carbon nanotubes pristine (doping free) and found that the variation of the gas flow changed the physical properties of nanotubes (length variation). They proposed that this is caused by the cooling rate of the substrate or the short time that the catalyst remain in the reactor [15].



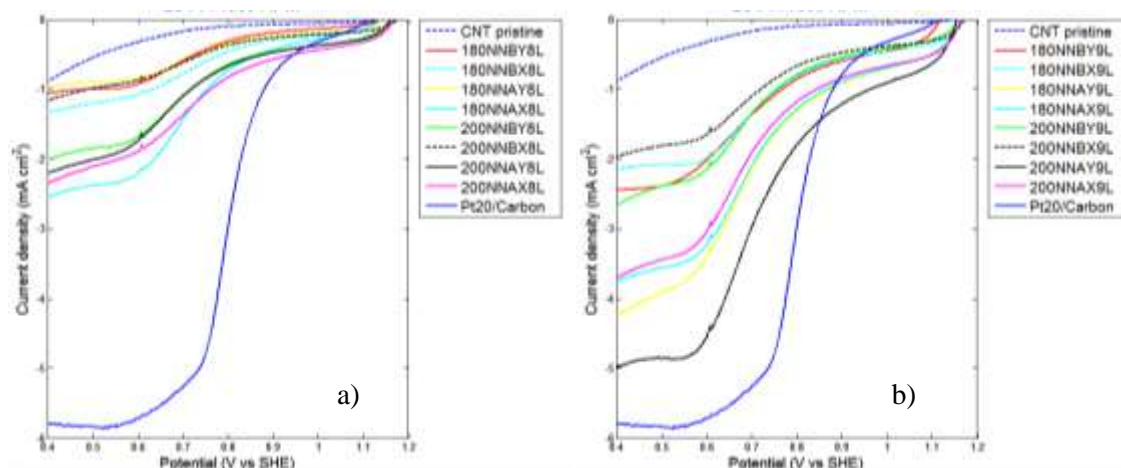


Figure 5. Oxygen reduction reaction curves a) N-CNTs at 800°C and b) N-CNTs at 900°C in O₂-saturated 0.5 M H₂SO₄ at 1600 rpm, $v = 5 \text{ mV s}^{-1}$.

The 200NNAY9L sample showed the highest current density limit in all the samples. Therefore, it was chosen to study the reaction kinetics for the ORR by RDE at different rotation speeds. As shown in Figure 6(a), the ORR current densities increase with increasing rotation speed. The kinetic parameter was analyzed using the Koutecky-Levich (K-L) equations.

$$\frac{1}{j} = \frac{1}{j_k} + \frac{1}{j_d} = \frac{1}{j_k} + \frac{1}{B\omega^{1/2}} \quad (1)$$

$$j_k = nFk_f C_o \quad (2)$$

$$j_d = 0.2nFD_o^{2/3}v^{-1/6}C_o \quad (3)$$

where j is the measured current density, j_k and j_d are the kinetic and diffusion limited current density respectively, k_f is the electrochemical rate constant for O₂ reduction, D is the diffusion coefficient of oxygen ($1.8 \times 10^{-5} \text{ cm}^2 \text{ s}^{-1}$), C_o is its concentration in the bulk ($1.13 \times 10^{-6} \text{ mol cm}^{-3}$) and v is the kinematic viscosity of the solution ($0.01 \text{ cm}^2 \text{ s}^{-1}$). The data are given for 0.5 M H₂SO₄[4].



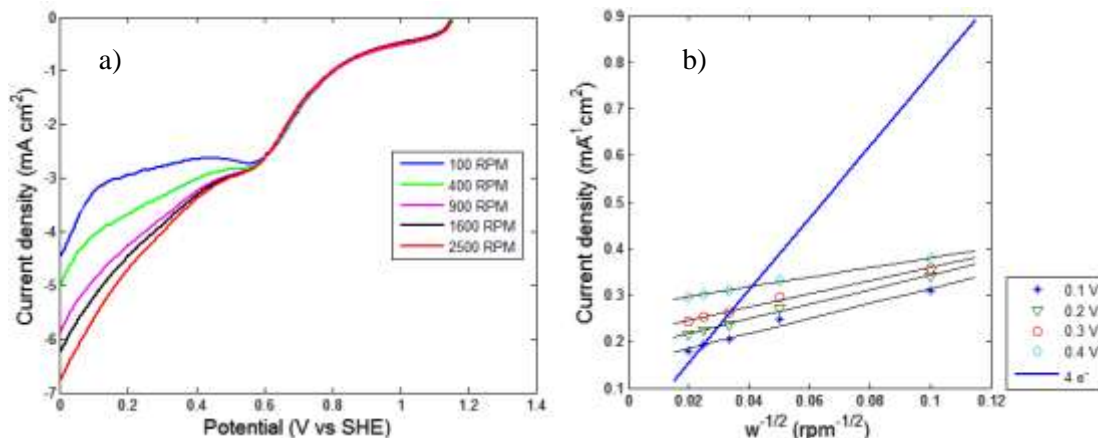


Figure 6. a) Polarization curves of oxygen reduction reaction (sample 200NNAY9L), O₂-saturated 0.5 M H₂SO₄ with different rotation speed at potential rate of 5 mV s⁻¹. b) Koutecky-Levich plot for ORR at various potentials.

The K-L plots of oxygen reduction on the 200NNAY9L sample are presented in Figure 6(b). The K-L lines show the good linearity and parallelism, indicating that the ORR process over the N-CNT electrocatalyst follows first-order kinetics in the selected potential range. The number of electrons transferred per O₂ molecule (*n*) was calculated from the slope of the K-L lines. The slope of the line of 200NNAY9L is slightly shifted to the theoretical line of four electrons. This could be result of the deviation in number of electrons transferred or slight deviation from the proposed first order kinetic [5]. The obtained result indicates that the ORR of N-CNT may not proceed preferably by a 4-electron process [20].

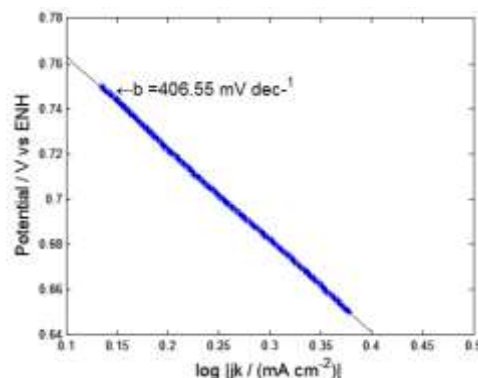


Figure 7. Tafel plot of ORR for 200NNAY9L (at 1600 rpm).

A more detailed comparison of the catalytic activity of the material can be obtained by the Tafel slope (Figure 7) which is obtained from the values of kinetic current density (*j_k*). The slope estimate for 200NNAY9L sample was 406 mV dec⁻¹, which is four times higher than the 20 wt. % Pt/C (104 mV dec⁻¹).



This value indicates that the reaction rate is slow on the sample. High slope (greater than 130 mV dec^{-1}) can be attributed to the blocking of active sites by the peroxide formed as an intermediate in the reaction [20, 21]. Although the lower electrocatalytic activity, this is an interesting non platinum material to be used in fuel cells electrodes.

4. Summary and perspectives

In this work the influence of synthesis parameters in N-CNTs synthesized with pyridine on the ORR performance were studied. The higher ORR activity was founded in the N-CNTs synthesized at 900°C and flow rate of 1 L/min . This activity could be attributed to higher content of nitrogen in the N-CNTs, which leads to increased disorder in structure. This proves that the nitrogen content plays an important role in the ORR activity. ORR kinetic analysis revealed that the N-CNTs has not yet reached the electrocatalytic properties of Pt/C, however shows a good electrochemical performance for a non-platinum catalysts. Finally, N-CNTs synthesized are suitable candidates for the ORR at the cathode of the fuel cell.

Acknowledgements

The authors acknowledge the financial support provided by FOMIX CONACYT - Estado de Quintana Roo, under project QR00-2011-001-174895. Also thanks to NANOTECH – CIMAV for technical support in HRTEM, Raman Spectroscopy and Thermogravimetric analysis.

References

- [1] Chen Zhu, Drew Higgins, Haisheng Tao, Ryan S. Hsu, and Zhongwei Chen. Highly Active Nitrogen-Doped Carbon Nanotubes for Oxygen Reduction Reaction in Fuel Cell Applications. *J. Phys. Chem. C* 2009, 113, 21008–21013.
- [2] Wong WY, Daud W.R.W., Mohamad A.B., Kadhum A.A.H. Influence of nitrogen doping on carbon nanotubes towards the structure, composition and oxygen reduction reaction. *International Journal of Hydrogen Energy* vol. 38 (2013) 9421-9430.
- [3] Wang Yongxia, Xiangzhi Cui, Yongsheng Li, Lisong Chen, Hangrong Chen, Lingxia Zhang, Jianlin Shi. A co-pyrolysis route to synthesize nitrogen doped multiwall carbon nanotubes for oxygen reduction reaction. *Carbon* vol. 68 (2014) 232-239.
- [4] Alexeyeva N., E. Shulga, V. Kisand, I. Kink, K. Tammeveski. Electroreduction of oxygen on nitrogen-doped carbon nanotube modified glassy carbon electrodes in acid and alkaline solutions. *Journal of Electroanalytical Chemistry* 648 (2010) 169–175.
- [5] Higgins Drew, Zhu Chen, Zhongwei Chen. Nitrogen doped carbon nanotubes synthesized from aliphatic diamines for oxygen reduction reaction. *Electrochimica Acta* 56 (2011) 1570–1575.
- [6] Xiong Chun, Zidong Wei, Baoshan Hu, Siguo Chen, Li Li, Lin Guo, Wei Ding, Xiao Liu, Weijia Ji, Xiaopei Wang. Nitrogen-doped carbon nanotubes as catalysts for oxygen reduction reaction. *Journal of Power Sources* 215 (2012) 216 - 220.
- [7] Maubane M. S., Messai A. Mamo, Edward N. Nxumalo, Willem A.L. Otterlo, Neil J. Coville. Tubular shaped composites made from polythiophene covalently linked to Prato functionalized N-doped carbon nanotubes. *Synthetic Metals* 162 (2012) 2307– 2315.
- [8] Higgins Drew C., Jason Wu, Wenmu Li, Zhongwei Chen. Cyanamide derived thin film on carbon nanotubes as metal free oxygen reduction reaction electrocatalyst. *Electrochimica Acta* 59 (2012) 8-13.
- [9] Choi Chang Hyuck, Seung Yong Lee, Sung Hyeon Park, Seonglhl Woo. Highly active N-doped-CNTs grafted on Fe/C prepared by pyrolysis of dicyandiamide on $\text{Fe}_2\text{O}_3/\text{C}$ for electrochemical oxygen reduction reaction. *Applied Catalysis B: Environmental* 103 (2011) 362–368.
- [10] Valenzuela Muñiz A.M., Y. Verde, M. Miki Yoshida, G. Alonso Nuñez. Synthesis of Multi-walled carbon nanotubes by spray-pyrolysis using a new iron organometallic complex as catalytic agent. *Journal of nanoscience and nanotechnology* 8 (2008) 6456-6460.



- [11] Alonso Nuñez G., A.M.ValenzuelaMuñiz, F. Paraguay Delgado, Y. Verde. New organometallic precursor catalysts applied to MWCNT synthesis by spray-pyrolysis. *Optical materials* 29 (2006) 134-139.
- [12] Zaiyong Mo, Shijun Liao, YuyingZheng, Zhiyong Fu. Preparation of nitrogen-doped carbon nanotube arrays and their catalysis towards cathodic oxygen reduction in acidic and alkaline media. *Carbon* vol. 50 (2012) 2620 - 2627.
- [13] Liu Jian, Yong Zhang, MihneaIoanIonescu, Ruying Li, Xueliang Sun. Nitrogen-doped carbon nanotubes with tunable structure and high yield produced by ultrasonic spray pyrolysis. *Applied Surface Science* 257 (2011) 7837–7844.
- [14] MhlangaSabelo D., Edward N. Nxumalo, Neil J. Coville, Vallabhapurapu V. Srinivasu. Nitrogen doping of CVD multiwalled carbon nanotubes: Observation of a large g-factor shift. *Materials Chemistry and Physics* 130 (2011) 1182– 1186.
- [15] Chaisitsak S., J. Nukeaw, A. Tuantranont. Parametric study of atmospheric-pressure single-walled carbon nanotubes growth by ferrocene–ethanol mist CVD. *Diamond & Related Materials* 16 (2007) 1958 - 1966.
- [16] B. Escobar, R. Barbosa, M. Miki Yoshida, Y. Verde Gomez. Carbon nanotubes as support of well dispersed platinum nanoparticles via colloidal synthesis. *Journal of Power Sources* 243 (2013) 88-94.
- [17] VikkiskM., IvarKruusenberg, UrmasJoost, Eugene Shulga, KaidoTammeveski. Electrocatalysis of oxygen reduction on nitrogen-containing multi-walled carbon nanotube modified glassy carbon electrodes. *ElectrochimicaActa*.Vol. 87 (2013) 709– 716.
- [18] DorjgotovAltansukh, Jinhee Ok, YuKwonJeon, Seong-Ho Yoon, Yong Gun Shul. Activity and active sites of nitrogen-doped carbon nanotubes or oxygen reduction reaction. *Journal ApplElectrochem* 43 (2013) 387 - 397.
- [19] QiuYeJun, Jing Yin, HuiwenHou, Jie Yu, XinbingZuo. Preparation of nitrogen-doped carbon submicrotubes by coaxial electrospinning and their electrocatalytic activity for oxygen reduction reaction in acid media.*ElectrochimicaActa*96 (2013) 225- 229.
- [20] Zinola C.F. Castro A.M., Triaca W.E., Arvía A.J. Kinetics and mechanism of the electrochemical reduction of molecular oxygen on platinum in KOH. *Journal Appl. Electrochem* 24 (1994) 531-541.
- [21] Yin Zhong-shu, Tian-hang Hu, Jian-long Wang, Cheng Wang, Zhi-xiang Liu, Jian-weiGuo.Preparation of highly active and stable polyaniline-cobalt-carbon nanotube electrocatalyst for oxygen reduction reaction in polymer electrolyte membrane fuel cell.*ElectrochimicaActa*119 (2014) 144– 154.

